

Article

# Shape Effects of Peptide Amphiphile Micelles for Targeting Monocytes

Johan Joo <sup>1,†</sup>, Christopher Poon <sup>1,†</sup>, Sang Pil Yoo <sup>2,3</sup> and Eun Ji Chung <sup>1,4,5,6,7,\*</sup>

<sup>1</sup> Department of Biomedical Engineering, University of Southern California, Los Angeles, CA 90089, USA; johanjoo@usc.edu (J.J.); poonc@usc.edu (C.P.)

<sup>2</sup> Institute for Molecular Engineering, University of Chicago, 5747 South Ellis Avenue, Chicago, IL 60637, USA; sangpilyoo@mednet.ucla.edu

<sup>3</sup> Current Affiliation: Medical Scientist Training Program, David Geffen School of Medicine, University of California, Los Angeles, Los Angeles, CA 90096, USA

<sup>4</sup> Mork Family Department of Chemical Engineering and Materials Science, University of Southern California, Los Angeles, CA 90089, USA

<sup>5</sup> Division of Nephrology and Hypertension, Department of Medicine, Keck School of Medicine, University of Southern California, Los Angeles, CA 90033, USA

<sup>6</sup> Norris Comprehensive Cancer Center, University of Southern California, Los Angeles, CA 90033, USA

<sup>7</sup> Department of Stem Cell Biology and Regenerative Medicine, University of Southern California, Los Angeles, CA 90033, USA

\* Correspondence: eunchung@usc.edu; Tel.: +1-213-740-2925

† These authors contributed equally to this work.

## Supplemental Figures

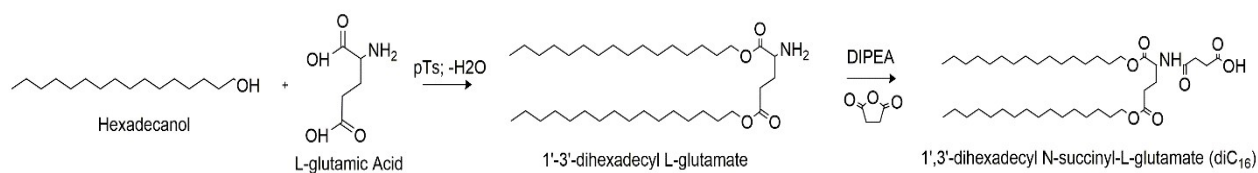


**Figure S1.** Synthesis of 1'-3'-dihexadecyl L-glutamate through an azeotropic distillation. The resulting product was deprotonated and a spacer molecule (succinic anhydride) was inserted to form the diC<sub>16</sub> tail.

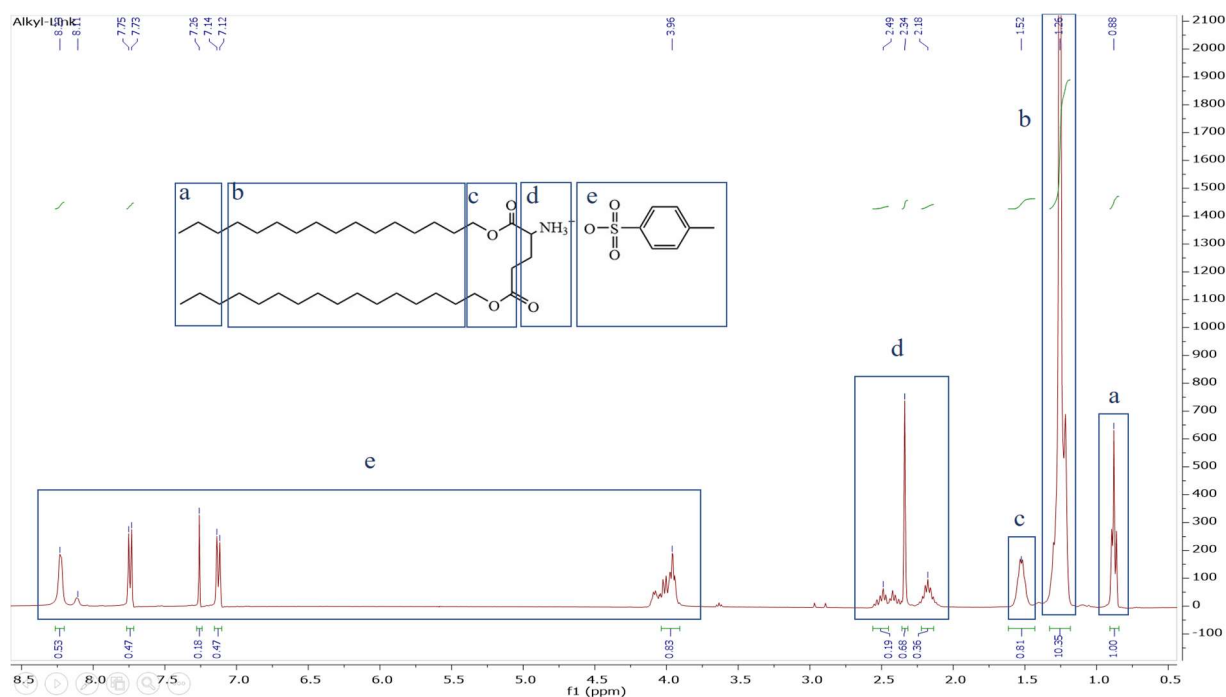


**Figure S2.** <sup>1</sup>H-NMR analysis of 1'-3'-dihexadecyl L-glutamate in CDCl<sub>3</sub>. The peaks within boxes correspond to a specific part of the compound structure.

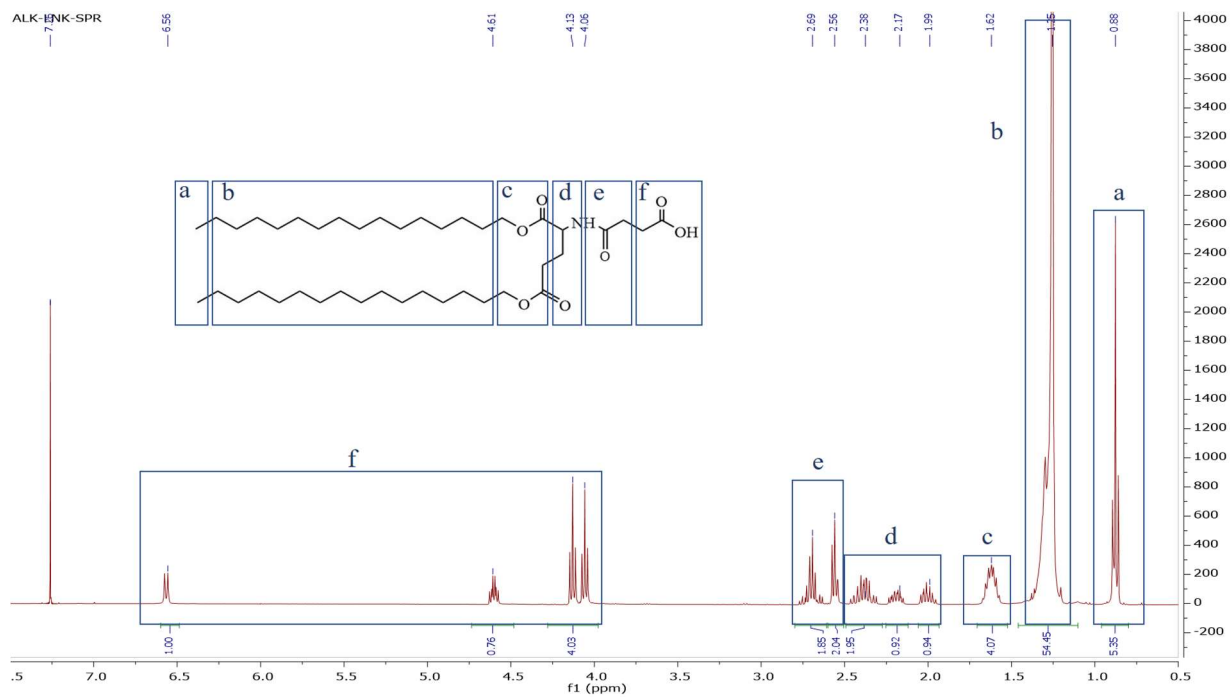


**Figure S3.**  $^1\text{H-NMR}$  analysis of diC<sub>16</sub> tail (1',3'-dihexadecyl N-succinyl-L-glutamate) in  $\text{CDCl}_3$ . The peaks within boxes correspond to a specific part of the compound structure.

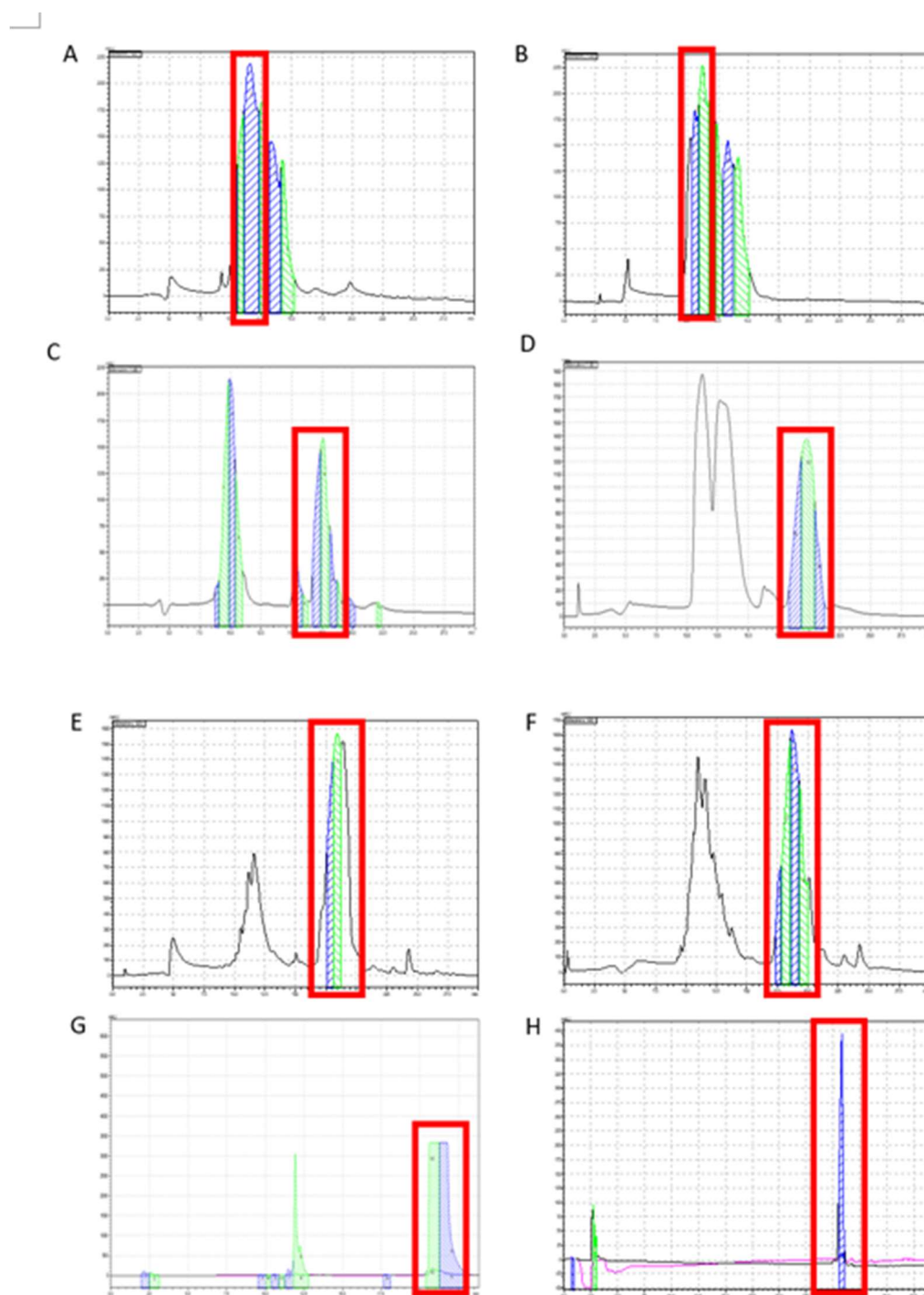


**Figure S4.** HPLC chromatogram of A) MCP-1 peptide, B) Scrambled peptide, C) DSPE-PEG<sub>2000</sub>-MCP-1, D) DSPE-PEG<sub>2000</sub>-Scrambled, E) diC16 MCP-1, F) diC16 Scrambled, G) DSPE-PEG<sub>2000</sub>-Cy7, and H) diC16-Cy7. The highlighted area (red box) were analyzed via MALDI (Figure S5-S12).

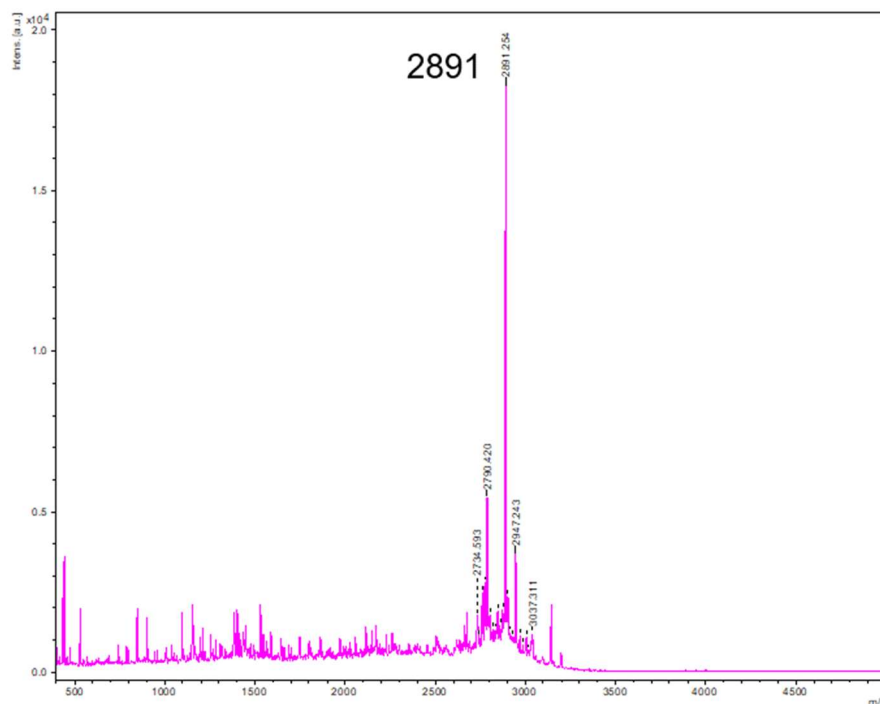


**Figure S5.** MALDI-TOF mass spectra of the MCP-1 peptide at a range of 400 – 5000 Da. Highest peak corresponds to  $[M + H]^+ = 2891$  (expected 2892).

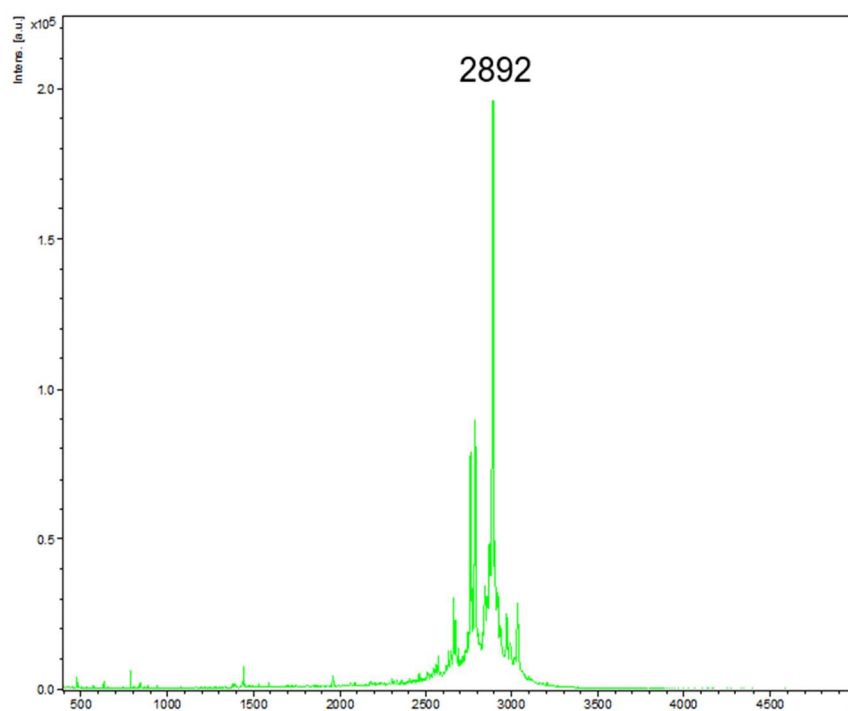


**Figure S6.** MALDI-TOF mass spectra of the scrambled MCP-1 peptide at a range of 450 – 5000 Da. Highest peak corresponds to  $[M + H]^+ = 2892$  (expected 2892).

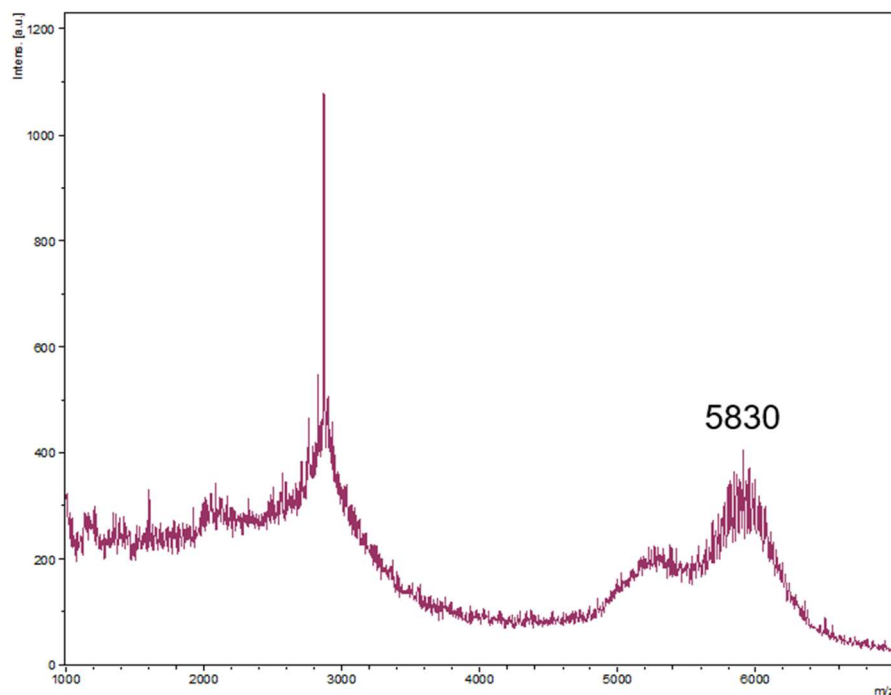


**Figure S7.** MALDI-TOF mass spectra of DSPE-PEG<sub>2000</sub> MCP-1 at a range of 1000 – 7000 Da. Rightmost peak corresponds to  $[M + H]^+ = 5830$  (expected 5830).

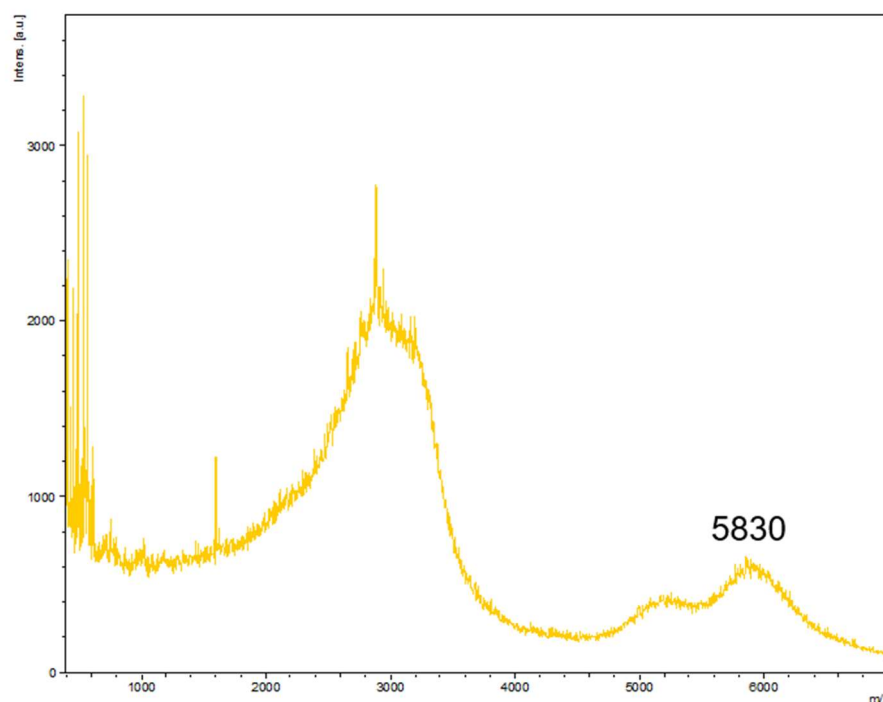


**Figure S8.** MALDI-TOF mass spectra of DSPE-PEG<sub>2000</sub> scrambled MCP-1 at a range of 400 – 7000 Da. Rightmost peak corresponds to  $[M + H]^+ = 5830$  (expected 5830).

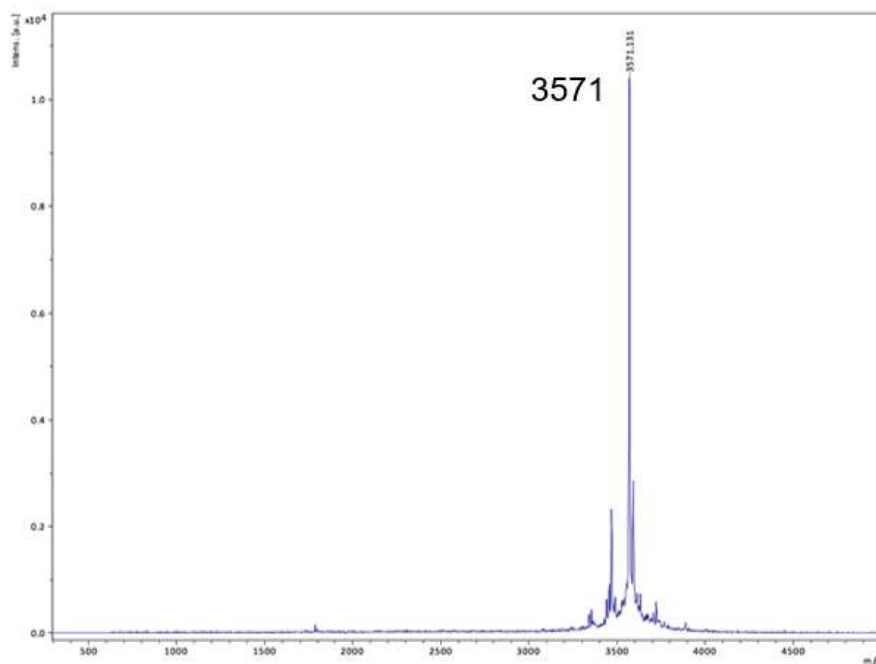


**Figure S9.** MALDI-TOF mass spectra of diC<sub>16</sub> MCP-1 at a range of 300 – 5000 Da. Highest peak corresponds to  $[M + H]^+ = 3571$  (expected 3571).

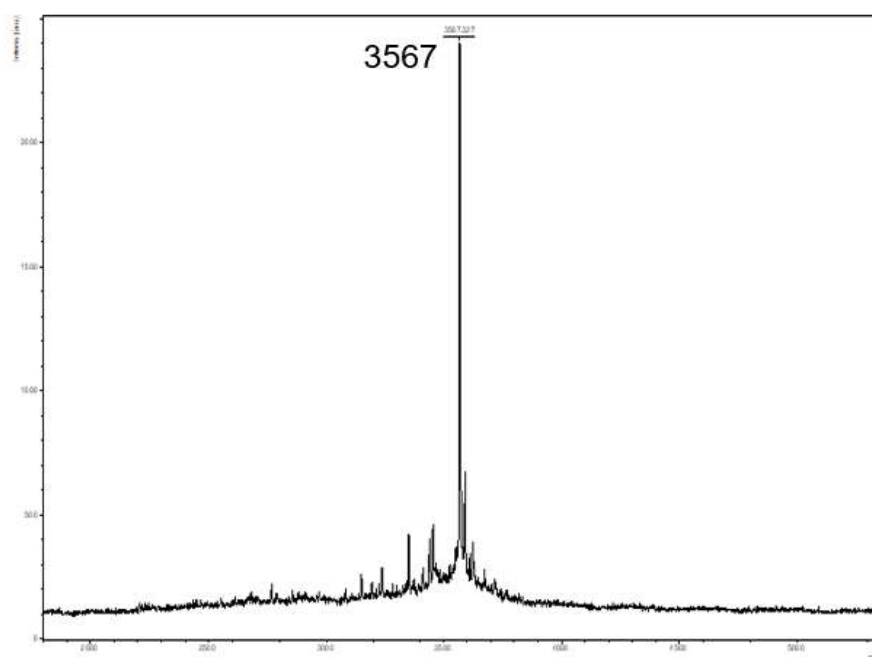


**Figure S10.** MALDI-TOF mass spectra of diC<sub>16</sub> scrambled MCP-1 at a range of 1800 – 5400 Da. Highest peak corresponds to  $[M + H]^+ = 3567$  (expected 3571).

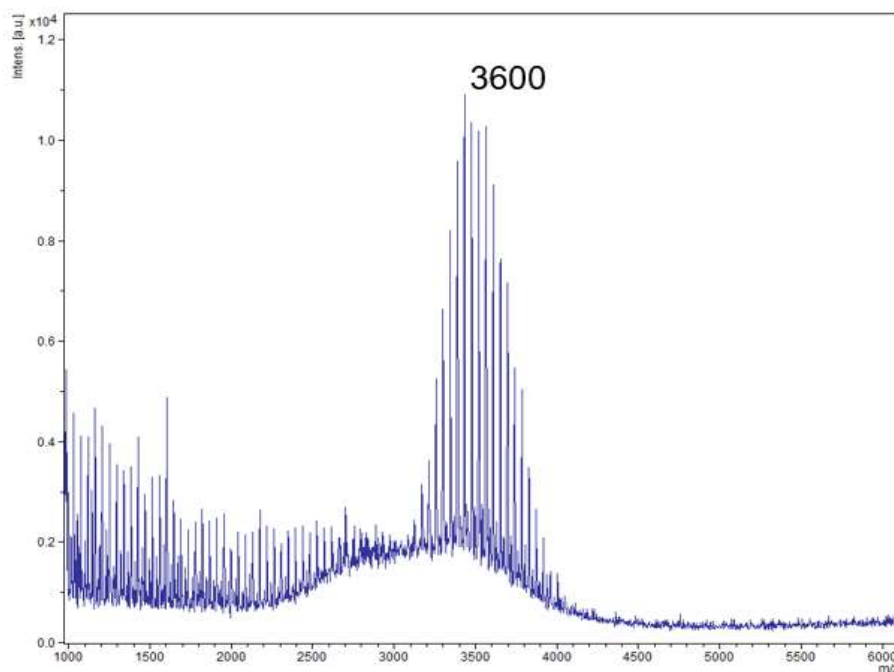


**Figure S11.** MALDI-TOF mass spectra of DSPE-PEG<sub>2000</sub> Cy7 at a range of 1000 – 6100 Da. Center peak corresponds to  $[M + H]^+ = 3600$  (expected 3680).

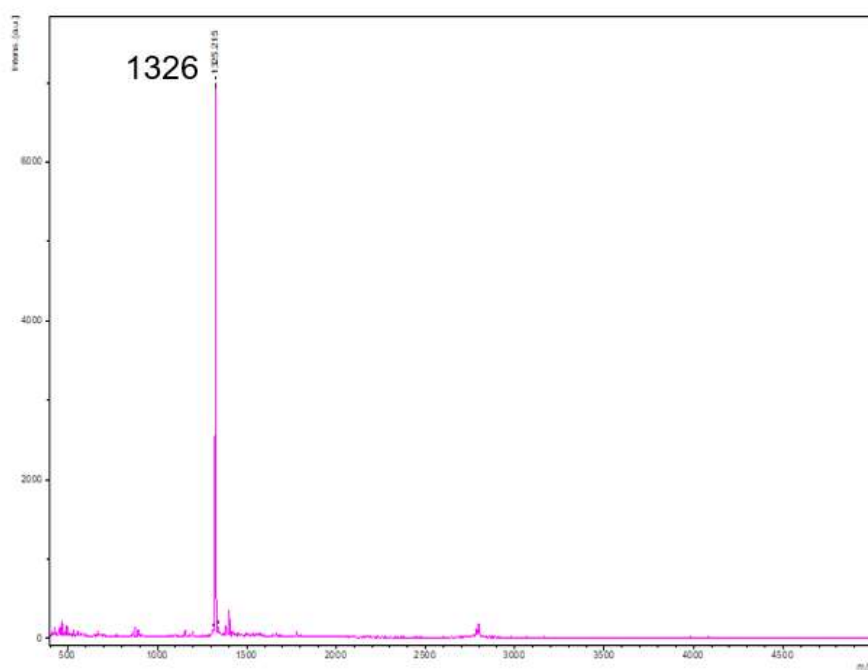


**Figure S12.** MALDI-TOF mass spectra of diC<sub>16</sub> Cy7 at a range of 400 – 5000 Da. Highest peak corresponds to  $[M + H]^+ = 1326$  (expected 1326).



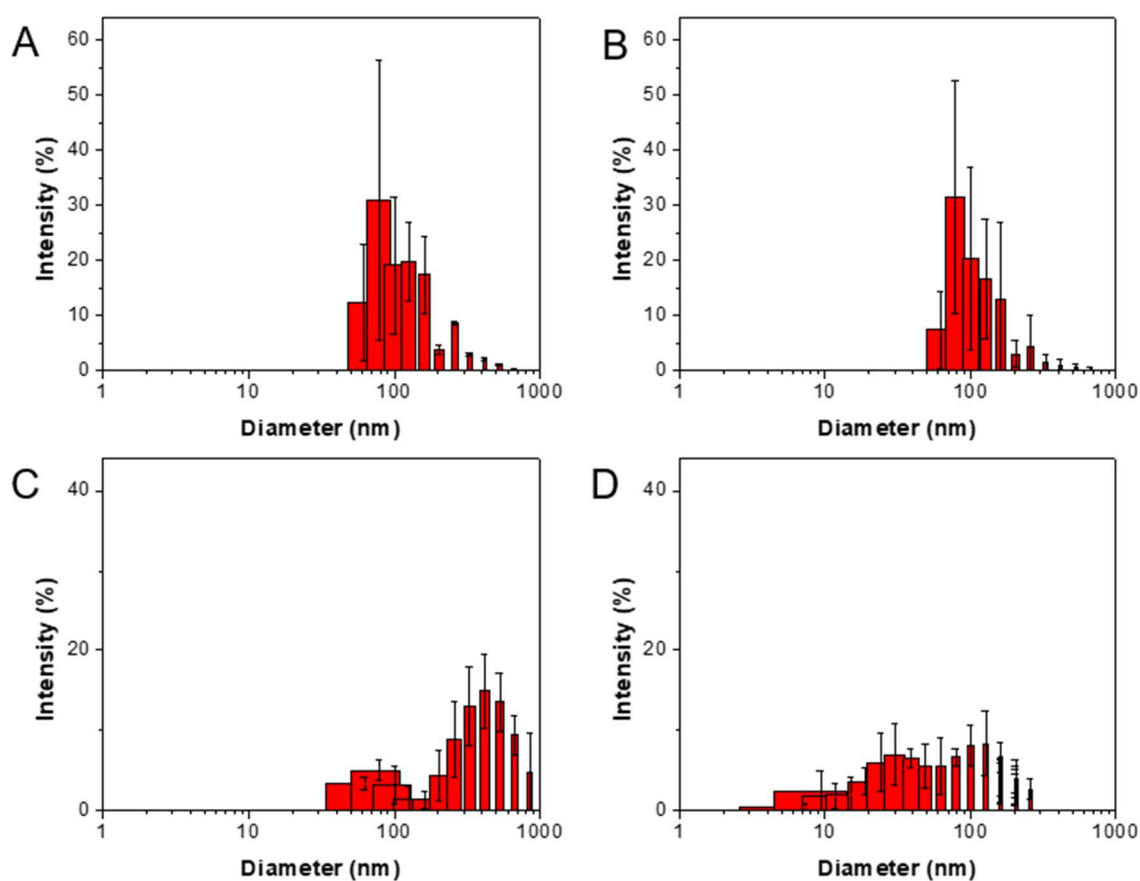


**Figure S13.** Dynamic light scattering (DLS) size intensity averages of A) S-MCP-1 PAMs, B) S-Scrambled PAMs, C) C-MCP-1 PAMs, and D) C-Scrambled PAMs.

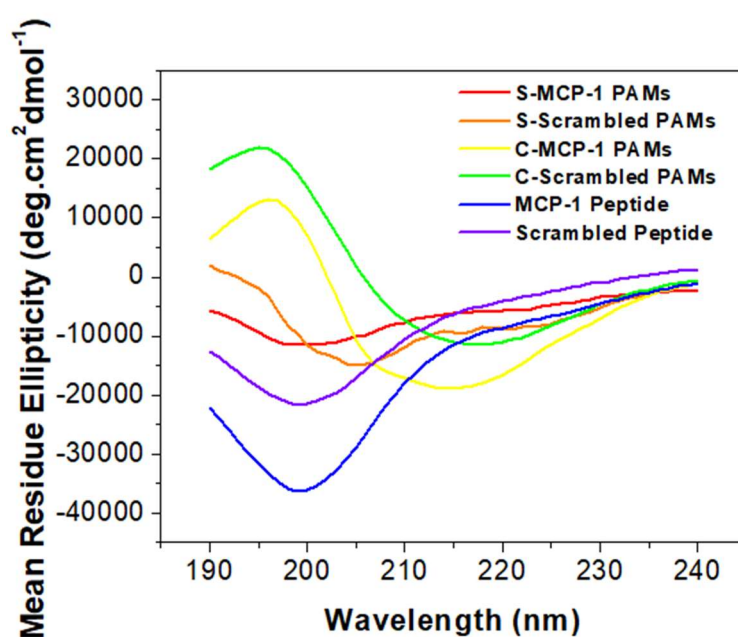


**Figure S14.** Circular dichroism spectroscopy of spherical MCP-1 PAMs (DSPE-PEG<sub>2000</sub> MCP-1 PAMs), scrambled spherical PAMs, cylindrical MCP-1 PAMs (diC<sub>16</sub> MCP-1 PAMs), scrambled cylindrical MCP-1 PAMs, MCP-1 peptides, and scrambled peptides.

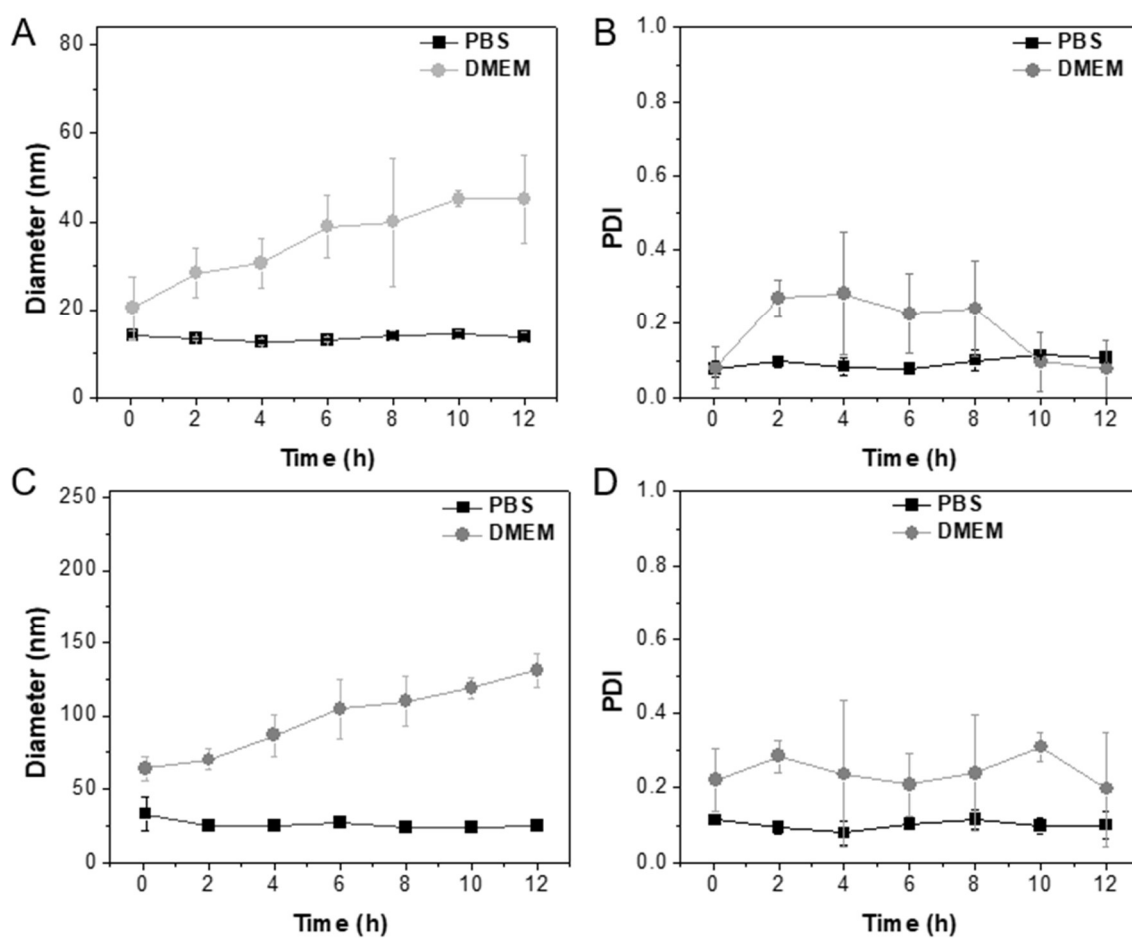


**Figure S15.** Particle stability of A) S-MCP-1 PAMs and C) C-MCP-1 PAMs measured by DLS, along with the polydispersity index (PDI) of B) S-MCP-1 PAMs and D) C-MCP-1 PAMs.